

# Cation...anion and anion...anion interactions compete in hydrogen-bonded frameworks prepared using amidinium...phosphonate hydrogen bonding

Phonlakrit Muang-Non<sup>a</sup> and Nicholas G. White<sup>\*a</sup>

<sup>a</sup> *Research School of Chemistry, Australian National University, Canberra, ACT, 2601, Australia*  
Email: [nicholas.white@anu.edu.au](mailto:nicholas.white@anu.edu.au), Website: [www.nwhitegroup.com](http://www.nwhitegroup.com)

We report the synthesis of hydrogen-bonded frameworks prepared from guanidinium, bis-amidinium or tetra-amidinium cations, and diphosphonate or tetraphosphonate anions. The frameworks are assembled by both charge-assisted amidinium...phosphonate and anti-electrostatic phosphonate...phosphonate hydrogen bonds, of which the phosphonate...phosphonate interactions are notably shorter. Frameworks prepared from the tetrahedral tetraphosphonate building block contain relatively large water-filled channels, but lose crystallinity upon drying. The crystal structure of a guanidinium...diphosphonate salt has an unusual structure related to classic Ward guanidinium...sulfonate frameworks but with an additional cation/solvent layer. This material includes toluene guests, which are held strongly within the crystal lattice.

## Introduction

Hydrogen-bonded frameworks are an emerging class of potentially porous materials.<sup>1,2</sup> Pioneering work in the early 1990s from Ermer<sup>3</sup> and Wuest's groups<sup>4,5</sup> showed that neutral molecules could be crystallised to give channel-containing network structures through self-complementary hydrogen bonding. Shortly after, Ward demonstrated that the assembly of guanidinium cations and polysulfonate anions could give a large family of frameworks, which could include a variety of guest molecules.<sup>6-9</sup> In the last decade or so, a huge number of reports of hydrogen bonded frameworks have been reported, which have been used for a variety of applications including gas sorption/separation,<sup>10-14</sup> sensing,<sup>15,16</sup> and enzyme encapsulation.<sup>17,18</sup>

Many of these frameworks have been assembled from a single neutral building block, however a significant amount of effort has been dedicated to assembling frameworks from two oppositely-charged building blocks.<sup>19,20</sup> These systems contain significantly stronger hydrogen bonds than those assembled from neutral components. However, this can come with drawbacks, with the need to use more polar solvents to dissolve the charged building blocks leading to difficulties in removing solvent from the frameworks without structural rearrangement.<sup>21-23</sup>

The vast majority of charge-assisted hydrogen-bonded frameworks have used either carboxylate<sup>24-26</sup> or sulfonate anions,<sup>6-9,23,27-30</sup> presumably because these remain deprotonated at neutral conditions and have (relatively) predictable hydrogen bonding geometries. In contrast, very little work has investigated the use of phosphonate anions for the assembly of hydrogen-bonded frameworks. Potentially, these would represent an interesting canvas for framework assembly, as phosphonate anions are able to undergo anti-electrostatic hydrogen bonding interactions<sup>31,32</sup> with one another in addition to interactions with the cation. Precedent for this approach exists in prior work which has shown that anti-electrostatically hydrogen

bonded pairs of bicarbonate anions can form frameworks with amidinium cations,<sup>33</sup> and that solution phase phosphonate...phosphonate interactions can be used to generate discrete and polymeric assemblies.<sup>34-36</sup>

We chose to use the amidinium...phosphonate pair to investigate possible framework formation. This pair of ions has been used in solution phase self-assembly,<sup>37-39</sup> and we are aware of three reports of its use to form hydrogen-bonded frameworks from 2D components.<sup>40-42</sup> In 2014, Wuest and co-workers studied the interaction of a bis-amidinium cation with ditopic and tritopic aryl phosphonates (Figure 1), forming tape and sheet-like structures.<sup>40</sup> In 2022, Zhang and co-workers studied the assembly of a different bis-amidinium cation (**amid<sub>phen</sub><sup>2+</sup>**, Figure 1) with a carboxylic acid substituted diphosphonate. They formed two different frameworks, depending on the protonation state of the carboxylic acid/carboxylate group, one of which contained small water-filled channels.<sup>41</sup> Very recently, Champness and co-workers reported the use of benzylic phosphonates, including one derived from naphthalenediimide in which the imide group ring-opened during crystallisation, to form hydrogen-bonded frameworks containing water-filled channels with **amid<sub>phen</sub><sup>2+</sup>**.<sup>42</sup> In addition to these frameworks, we are aware of two structures assembled from di- or triphosphonates and guanidinium cations,<sup>43,44</sup> although these are both densely-packed (guanidinium, **guan<sup>+</sup>**, is an amidinium cation containing a third NH<sub>2</sub> group, Figure 1).

In this work, we study the assembly of poly-amidinium cations and poly-phosphonate anions including 3D tetrahedral tectons, and investigate their ability to form porous framework structures. We show that it is possible to form open frameworks with some degree of predictability, although the stability of these materials to drying is limited. We also report the crystal structure of a pillared network from **guan<sup>+</sup>** cations and a diphosphonate anion, which represents an unusual variation of the classic Ward guanidinium...sulfonate framework motif.<sup>6</sup>

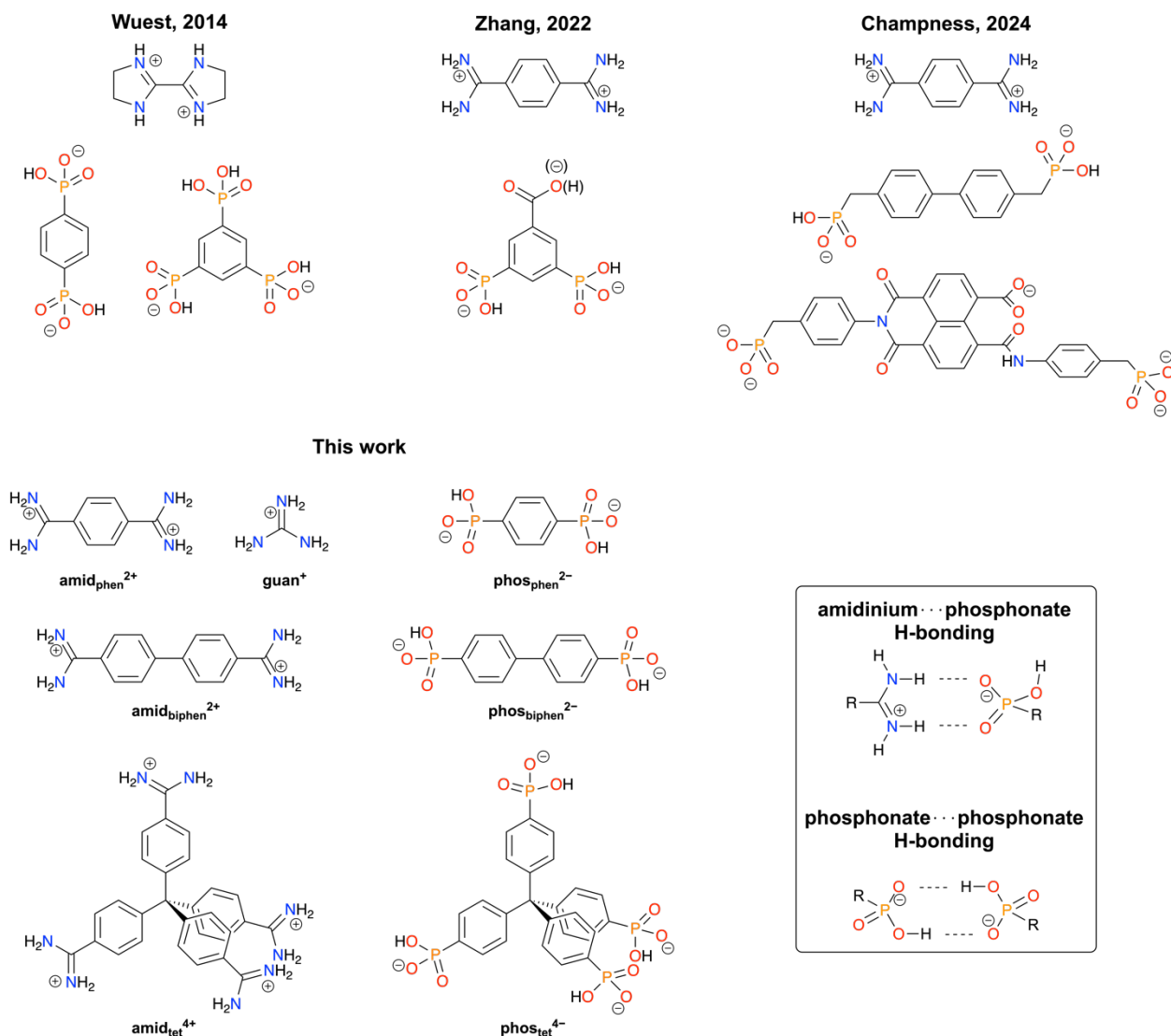


**Figure 1** Structures of the building blocks used by Wuest and co-workers,<sup>40</sup> Zhang and co-workers,<sup>41</sup> and Champness and co-workers<sup>42</sup> to prepare hydrogen bonded frameworks, and structures of the building blocks used in the current work. Note that Zhang prepared two frameworks, one of which contained the 2<sup>-</sup> form of their building block where the carboxylic acid remained protonated, and one which contained the 3<sup>-</sup> form with a deprotonated carboxylate group. Possible hydrogen bonding interactions are shown inset; these are shown interacting in a  $R_2^2(8)$  manner (in graph set notation<sup>45</sup>), but other hydrogen bonding interactions are also possible.

## Results and discussion

### Synthesis of tectons

The building blocks used in this work are shown in Figure 1. The tetraphenylmethane, biphenyl and phenyl-derived amidinium building blocks **amid<sub>tet</sub><sup>4+</sup>·Cl<sub>4</sub>**,<sup>21</sup> **amid<sub>biphen</sub>·Cl<sub>2</sub>**<sup>46</sup> and **amid<sub>phen</sub>·Cl<sub>2</sub>**<sup>47</sup> were synthesised as described previously. The guanidinium salt **guan·Cl** was purchased commercially. The phenyl, biphenyl, and tetraphenyl-derived phosphonic acids **phos<sub>phen</sub><sup>2H</sup>**,<sup>48</sup> **phos<sub>biphen</sub><sup>2H</sup>**<sup>49</sup> and **phos<sub>tet</sub><sup>4H</sup>**<sup>50</sup> were prepared following literature procedures. We prepared the tetrabutylammonium (TBA) salts of **phos<sub>biphen</sub><sup>2-</sup>** and **phos<sub>tet</sub><sup>4-</sup>** (i.e. **TBA<sub>2</sub>·phos<sub>biphen</sub>** and **TBA<sub>4</sub>·phos<sub>tet</sub>**) by reaction of **phos<sub>biphen</sub><sup>2H</sup>** and **phos<sub>tet</sub><sup>4H</sup>** with TBA·OH, however attempts to prepare **TBA<sub>2</sub>·phos<sub>phen</sub>** gave

only oily material that was difficult to work with, so we instead used **phos<sub>phen</sub><sup>2H</sup>** for crystallisation studies.

### Hydrogen-bonded assembly

Numerous crystallisation experiments were set up to try and crystallise various combinations of the building blocks shown in Figure 1. These were all conducted by mixing a solution of the amidinium tecton with a solution of the polyphosphonate tecton and leaving the mixture to stand at room temperature. Using this approach we were able to obtain single crystals of **amid<sub>phen</sub>·phos<sub>phen</sub>**, **amid<sub>biphen</sub>·phos<sub>phen</sub>**, **(amid<sub>phen</sub>)<sub>2.5</sub>·phos<sub>tet</sub><sup>-1.5H</sup>**, **(amid<sub>biphen</sub>)<sub>3</sub>·phos<sub>tet</sub><sup>-2H</sup>**, **amid<sub>tet</sub>·phos<sub>tet</sub>** and **(guan)·phos<sub>biphen</sub>**, although several other combinations

proved resistant to crystallisation. These structures are described in turn, followed by a brief discussion section, describing the structures together. Full details of conditions that did and did not lead to crystallisation are provided in the SI.

### Crystal structures of salts of bis-amidiniums and diphosphonates

Before attempting to synthesise three-dimensional framework structures, we studied the interaction of the simple ditopic amidiniums **amid<sub>phen</sub><sup>2+</sup>** and **amid<sub>biphen</sub><sup>2+</sup>** with the diphosphonates **phos<sub>phen</sub><sup>2-</sup>** and **phos<sub>biphen</sub><sup>2-</sup>**. We did not obtain any crystal structures containing **phos<sub>biphen</sub><sup>2-</sup>** but were able to crystallise **amid<sub>phen</sub>·phos<sub>phen</sub>** and **amid<sub>biphen</sub>·phos<sub>phen</sub>**. Both of these salts crystallised upon mixing the chloride salt of the bis-amidinium and the phosphonic acid containing **phos<sub>phen</sub><sup>2H</sup>** in water. In both cases, deprotonation of the phosphonic acid building block occurred spontaneously. The salts were isolated and characterised by <sup>1</sup>H NMR spectroscopy of the acid-digested salt, powder X-ray diffraction (PXRD), thermogravimetric analysis (TGA) and IR spectroscopy (Supporting Information). All characterisation data was consistent with the structures determined by single crystal X-ray diffraction (SCXRD) studies.

**Crystal structure of amid<sub>phen</sub>·phos<sub>phen</sub>:** The structure of **amid<sub>phen</sub>·phos<sub>phen</sub>** crystallises as the dihydrate, with each **phos<sub>phen</sub><sup>2H</sup>** losing two protons to form **phos<sub>phen</sub><sup>2-</sup>** during crystallisation. Phosphonic acids are highly acidic, so it is perhaps unsurprising that a proton is lost. We have also observed evidence for deprotonation of R-PO<sub>3</sub>H<sup>-</sup> groups (see later), as has previously been observed by Champness in related systems.<sup>42</sup> These deprotonations are not particularly surprising given the pK<sub>a</sub> of phosphonic acid and phosphonate groups (e.g. pK<sub>a</sub> of Ph-PO<sub>3</sub>H<sub>2</sub> = 1.4, pK<sub>a</sub> of Ph-PO<sub>3</sub>H<sup>-</sup> = 6.9<sup>52</sup>).

The structure of **amid<sub>phen</sub>·phos<sub>phen</sub>** features short “paired” *R*<sub>2</sub><sup>2</sup>(8) anti-electrostatic hydrogen bonds between phosphonate anions (H...O distance = 1.72 Å). These interactions are significantly shorter than other hydrogen bonding interactions, which occur from water or amidinium groups with the phosphonate anion (water H...O distance = 1.86 Å; amidinium H...O distance = 2.02 Å, Figure 2).

**Crystal structure of amid<sub>biphen</sub>·phos<sub>phen</sub>:** The structure of **amid<sub>biphen</sub>·phos<sub>phen</sub>** is quite different to that containing the smaller **amid<sub>phen</sub><sup>2+</sup>** building block. It is assembled from 1D hydrogen-bonded chains made up of *R*<sub>2</sub><sup>2</sup>(8) amidinium...phosphonate hydrogen bonds (H-O distances: 2.06 – 2.12 Å). These then link into 2D sheets through C(4) anti-electrostatic hydrogen bonding between phosphonate groups (H-O distances: 1.74 – 1.75 Å, Figure 3).<sup>51</sup> There are small 1D channels in the structure, which are filled with water molecules (two water molecules per

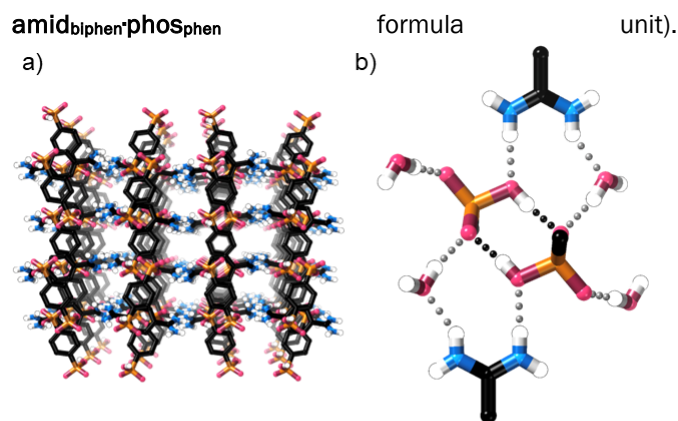


**Figure 2** Crystal structure of **amid<sub>phen</sub>·phos<sub>phen</sub>**: a) packing diagram (water molecules and C-H hydrogen atoms omitted for clarity); b) diagram showing hydrogen bonding interactions.

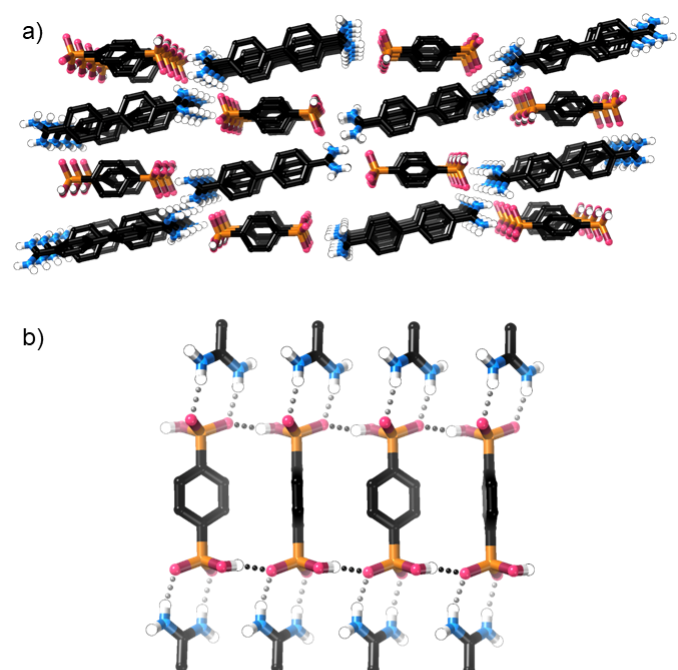


**Figure 3** Crystal structure of **amid<sub>biphen</sub>·phos<sub>phen</sub>**: a) packing diagram; b) diagram showing hydrogen bonding interactions. Positional disorder of phenyl groups, C-H hydrogen atoms, and water molecules are omitted in both cases.

We were interested to see if these water molecules could be removed from the framework and if this resulted in structural rearrangement. Three dimensional frameworks assembled through amidinium...carboxylate<sup>21</sup> and amidinium...sulfonate<sup>22</sup> hydrogen bonds have been shown to re-arrange in a single-crystal-to-single-crystal manner upon removal of water molecules and so we were interested to see how structures built from amidinium...phosphonate interactions compared. TGA confirmed the presence of two water molecules per formula unit at room temperature, and revealed that these were lost upon heating to 80 °C. We were able to obtain a low quality X-ray crystal structure by

heating a single crystal to 80 °C; while data are of low quality, this revealed that water is lost in a single-crystal-to-single-crystal transition to a densely-packed phase (see SI for more information, and Figure S31 for a comparison of the low and high temperature phases). Variable temperature PXRD experiments show that this phase change also occurs in the bulk material upon heating (Figure S32).

### Three-dimensional hydrogen-bonded frameworks

We next studied the synthesis of frameworks containing the 3D tetrahedral building block **phos<sub>tet</sub><sup>4-</sup>**. Using various crystallisation conditions, we were able to obtain single crystals of **(amid<sub>phen</sub>)<sub>2.5</sub>·phos<sub>tet</sub><sup>-1.5H</sup>**, **(amid<sub>biphen</sub>)<sub>3</sub>·phos<sub>tet</sub><sup>-2H</sup>** and **amid<sub>tet</sub>·phos<sub>tet</sub>**.

**Crystal structure of (amid<sub>phen</sub>)<sub>2.5</sub>·phos<sub>tet</sub><sup>-1.5H</sup>:** We were able to obtain a few crystals of this compound from 1:1 methanol:water. Even though a 2:1 ratio of **amid<sub>phen</sub><sup>2+</sup>·phos<sub>tet</sub><sup>4-</sup>** was used in the crystallisation, the crystals have a 2.5:1 ratio of these building blocks. We determined the unit cell parameters of seven different single crystals, all of which were consistent with **(amid<sub>phen</sub>)<sub>2.5</sub>·phos<sub>tet</sub><sup>-1.5H</sup>**. However, <sup>1</sup>H NMR spectroscopy of the acid-digested bulk product suggests that these crystals are not representative of the bulk. It appears that as well as the single crystals there is a significant amount of microcrystalline material that has a different formulation and is too small for structure determination using SCXRD techniques.

The presence of 2.5 **amid<sub>phen</sub><sup>2+</sup>** cations, implies that the **phos<sub>tet</sub>** anion should have a 5<sup>-</sup> charge, *i.e.* **TBA<sub>4</sub>·phos<sub>tet</sub>** has lost a proton during crystallisation. However, the crystal structure shows that three of the phosphonate groups are forming short phosphonate...phosphonate hydrogen bonding interactions with an adjacent **phos<sub>tet</sub>** anion, with the hydrogen atom located on symmetry positions between the phosphonate groups. Therefore, each of these phosphonate groups has a 1.5<sup>-</sup> charge; the fourth phosphonate group is a conventional R-PO<sub>3</sub>H<sup>-</sup> group, meaning that overall the anion is **phos<sub>tet</sub><sup>5.5-</sup>** and the structure is not charge-balanced. We have searched the structure carefully to find an additional site for 0.5 of a hydrogen atom on a phosphonate group to give a charge-balanced structure, but cannot find a plausible position. We suggest that the most likely explanation is that either one of the amidinium groups is partially deprotonated, or there is a partial occupancy hydroxide group located in the water-filled channels. Unfortunately, because we were not able to prepare this framework cleanly in bulk, we were not able to investigate this using techniques other than X-ray crystallography.

The hydrogen bonding interactions between phosphonate groups are very short (O...O distances = 2.460(3) – 2.487(3) Å, hydrogen atoms are located on symmetry positions halfway between the two oxygen

atoms), and link the **phos<sub>tet</sub><sup>5.5-</sup>** anions into a two-dimensionally connected network containing quite large channels (Figure 4a). These channels contain **amid<sub>phen</sub><sup>2+</sup>** cations as well as water molecules, some of which were poorly-resolved and were included in the model using PLATON-SQUEEZE.<sup>53</sup> The amidinium cations all hydrogen bond to phosphonate groups, primarily through single-point D hydrogen bonding interactions (H...O distances = 1.95 – 2.23 Å), although there is one paired *R*<sub>2</sub><sup>2</sup>(8) interaction (H...O distances = 1.95, 1.95 Å). These hydrogen bonding interactions link the 2D networks of **phos<sub>tet</sub><sup>5.5-</sup>** anions into three dimensions (Figure 4b).

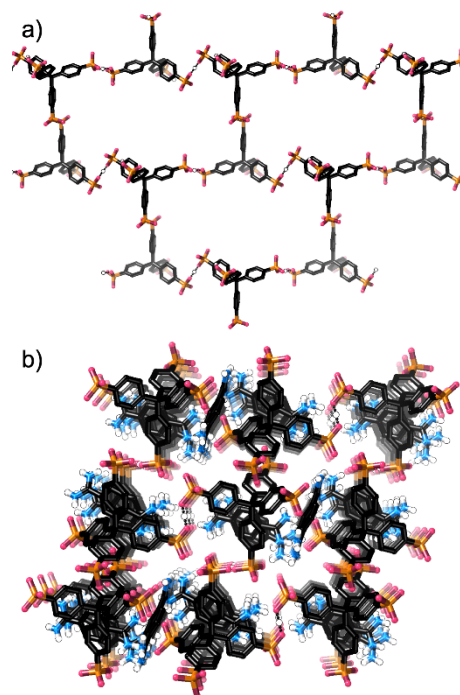


**Figure 4** Crystal structure of **(amid<sub>phen</sub>)<sub>2.5</sub>·phos<sub>tet</sub><sup>-1.5H</sup>**: a) diagram showing 2D hydrogen-bonded sheets formed from anti-electrostatic interactions between **phos<sub>tet</sub><sup>5.5-</sup>** units; b) packing diagram with water molecules omitted. C–H hydrogen atoms are omitted for clarity, PLATON-SQUEEZE<sup>53</sup> was used.

**Crystal structure of (amid<sub>biphen</sub>)<sub>3</sub>·phos<sub>tet</sub><sup>-2H</sup>:** We were able to obtain a small number of crystals from the crystallisation of **amid<sub>biphen</sub><sup>2+</sup>** and **phos<sub>tet</sub><sup>4-</sup>** in water. As was the case with the analogous crystallisation involving **amid<sub>phen</sub><sup>2+</sup>**, only a small number of crystals were obtained, the identity of these did not match that of the bulk material, and spontaneous deprotonation of **phos<sub>tet</sub><sup>4-</sup>** has occurred. In this case, the tetraphosphonate is in its 6<sup>-</sup> form, with two R-PO<sub>3</sub>H<sup>-</sup> groups and two R-PO<sub>3</sub><sup>2-</sup> groups. Both R-PO<sub>3</sub>H<sup>-</sup> groups form short hydrogen bonds to R-PO<sub>3</sub><sup>2-</sup> groups (H...O distances = 1.69, 1.82 Å), and there are a large number of hydrogen bonds between amidinium groups and phosphonate groups, which have D, *R*<sub>1</sub><sup>1</sup>(6) and *R*<sub>2</sub><sup>2</sup>(8) arrangements (H...O distances = 1.78 – 2.35 Å). Overall, these various hydrogen bonds link the structure into three dimensions and result in relatively large channels (Figure 5), which are filled with

poorly-resolved/disordered water molecules. These could not be refined sensibly and so the OLEX2 mask routine<sup>54</sup> was used to include their electron density in the refinement.

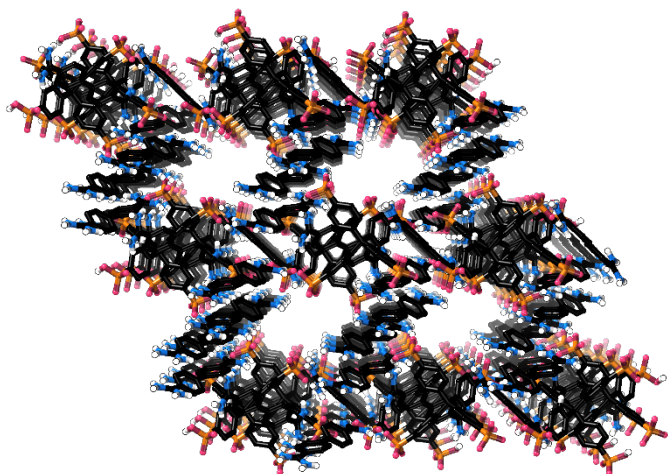


**Figure 5** Crystal structure of  $(\text{amid}_{\text{biphen}})_3 \cdot \text{phos}_{\text{tet}} \cdot 2\text{H}$  showing the relatively large channels. C–H hydrogen atoms are omitted for clarity; the OLEX2 solvent mask routine<sup>54</sup> was used.

**Crystal structure of  $\text{amid}_{\text{tet}} \cdot \text{phos}_{\text{tet}}$ :** We obtained very small crystals of  $\text{amid}_{\text{tet}} \cdot \text{phos}_{\text{tet}}$  by mixing the two components in water; SCXRD studies using synchrotron radiation revealed that these had the formula  $\text{amid}_{\text{tet}} \cdot \text{phos}_{\text{tet}}$ . Unlike the crystal structures of  $(\text{amid}_{\text{phen}})_2 \cdot 2.5 \cdot \text{phos}_{\text{tet}} \cdot 1.5\text{H}$  and  $(\text{amid}_{\text{biphen}})_3 \cdot \text{phos}_{\text{tet}} \cdot 2\text{H}$ , no spontaneous deprotonation of the phosphonate building block has occurred in the current structure. In this case, we were able to isolate  $\text{amid}_{\text{tet}} \cdot \text{phos}_{\text{tet}}$  on reasonable scales and show using <sup>1</sup>H NMR spectroscopy of an acid-digested sample, as well as IR spectroscopy, PXRD and TGA that the bulk material was consistent with the structure determined by X-ray crystallography (see SI).

The asymmetric unit of  $\text{amid}_{\text{tet}} \cdot \text{phos}_{\text{tet}}$  contains two complete molecules of both  $\text{amid}_{\text{tet}}^{4+}$  and  $\text{phos}_{\text{tet}}^{4-}$ , and there are a wide variety of amidinium...phosphonate (H...O distances = 1.88 – 2.18 Å) and phosphonate...phosphonate hydrogen bonds (H...O distances = 1.72 – 1.83 Å) that assemble a three dimensional network. There are also several hydrogen bonding interactions with well-resolved water molecules, although numerous other water molecules could not be refined sensibly and were included in the model using the OLEX2 solvent mask routine.<sup>54</sup> The structure contains large channels (Figure 6, approximately 11 × 6 Å between opposite sides). We were interested to see whether the structures were stable to evacuation as

related frameworks prepared from  $\text{amid}_{\text{tet}}^{4+}$  and the carboxylate<sup>21</sup> or sulfonate analogues of  $\text{phos}_{\text{tet}}^{4-}$ <sup>22,30</sup> adsorb water significant amounts of water vapour, which occurs with significant structural rearrangement. Unfortunately,  $\text{amid}_{\text{tet}} \cdot \text{phos}_{\text{tet}}$  becomes amorphous on drying, so we were unable to study this.

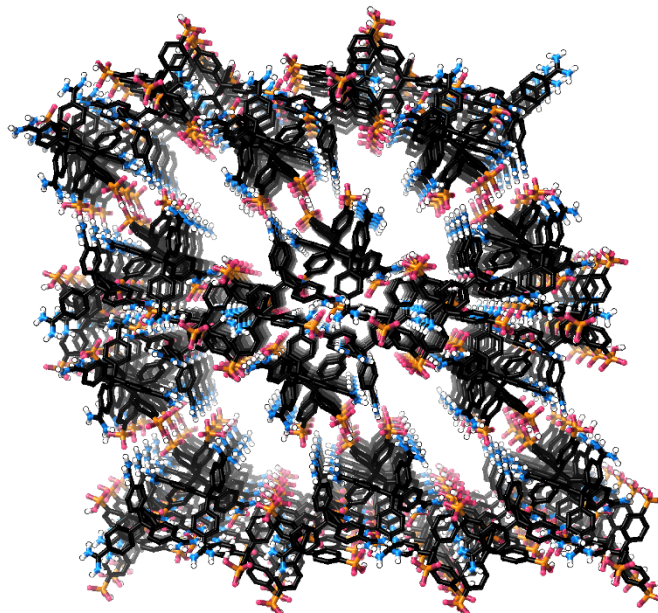


**Figure 6** Crystal structure of  $\text{amid}_{\text{tet}} \cdot \text{phos}_{\text{tet}}$  showing the relatively large channels. C–H hydrogen atoms are omitted for clarity; the OLEX2 solvent mask routine<sup>54</sup> was used.

### A pillared guanidinium...phosphonate structure

Inspired by Ward's studies on guanidinium...sulfonate frameworks,<sup>7,55</sup> we investigated the crystallisation of guanidinium cations with diphosphonate anions. We hoped that we would be able to form similar pillared bilayer structures to Ward, but potentially with additional anti-electrostatic hydrogen bonding interactions between phosphonate groups to further stabilise the structures. Initial attempts to prepare crystals by mixing the two components in water, or mixture of organic solvents and water were unsuccessful; however, mixing **guan·Cl** and **TBA<sub>2</sub>·phos<sub>biphen</sub>** in 1:1 methanol:toluene resulted in the formation of small single crystals of **guan<sub>2</sub>·phos<sub>biphen</sub>** over long periods (1 – 2 months), and we were able to characterise these by synchrotron X-ray crystallography. Analysis by <sup>1</sup>H NMR and IR spectroscopy, PXRD and TGA was consistent with the bulk product having the same structure as the single crystals (see SI).

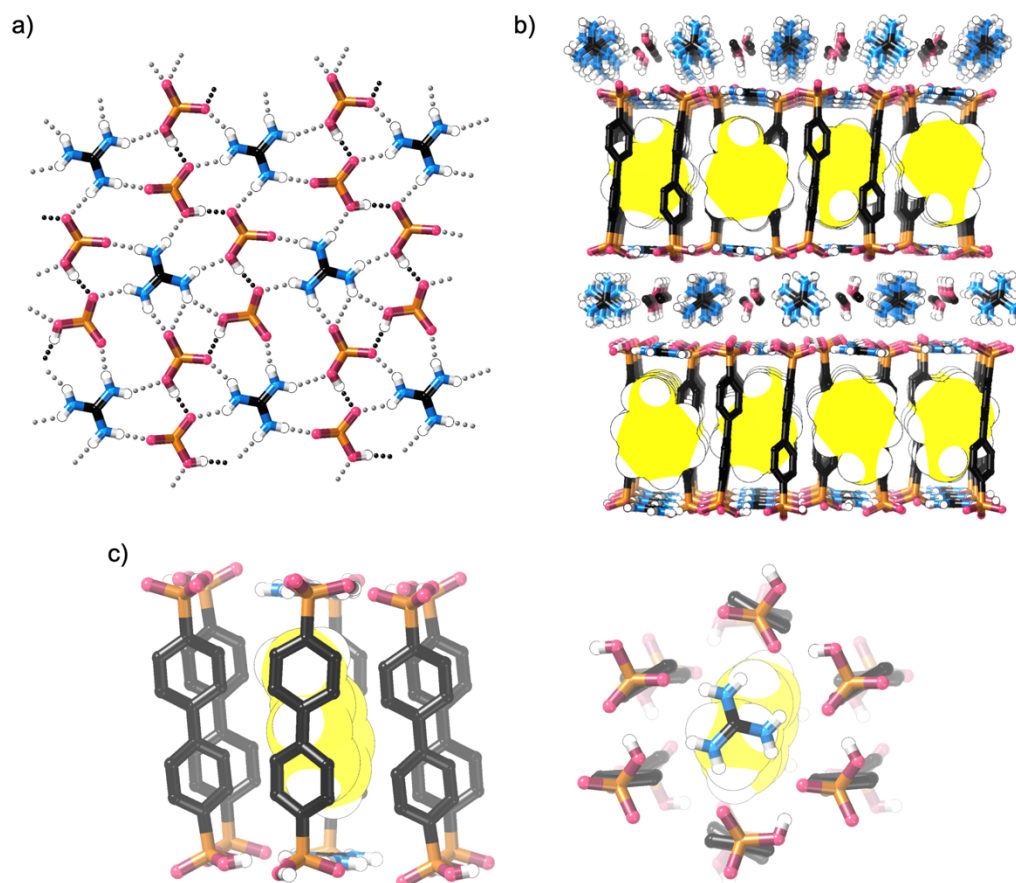


**Figure 7** Crystal structure of **guan<sub>2</sub>-phos<sub>biphen</sub>**: a) view of the 2D hydrogen-bonded sheets, b) packing diagram, c) two views of hexagonal “cage” encapsulating toluene guest. C–H hydrogen atoms on **phos<sub>biphen</sub><sup>2-</sup>** anions and methanol solvents omitted for clarity, toluene guests shown in yellow in space-filling representation.

The structure is shown in Figure 7, and is quite different from structures formed from the analogous sulfonate biphenyl-4,4'-disulfonate (*i.e.* **sulf<sub>biphen</sub><sup>2-</sup>**). Many structures of **guan<sub>2</sub>-sulf<sub>biphen</sub>** have been reported, which vary depending on the nature of the included guest, but they are characterised by charge-neutral hydrogen-bonded sheets made up of guanidinium cations and sulfonate groups.<sup>6,7,55,56</sup> In contrast, **guan<sub>2</sub>-phos<sub>biphen</sub>** contains 2D sheets that contain two mono-anionic phosphonate groups for each guanidinium cation. These are assembled through both guanidinium...phosphonate hydrogen bonds (H–O distances: 1.96 – 2.36 Å) and phosphonate...phosphonate interactions (H–O distances: 1.70, 1.70 Å). These sheets possess a negative charge, which is balanced by a cationic layer made up of guanidinium cations and methanol solvent molecules.

Toluene guests are included in the framework and are located in pseudo-hexagonal “cages” formed by six **biphen<sup>2-</sup>** groups. This arrangement is quite different from the analogous sulfonate-based material (*i.e.* **guan<sub>2</sub>-sulf<sub>biphen</sub>-toluene**) where the toluene guests are located in continuous channels, with each toluene close to four **sulf<sub>biphen</sub><sup>2-</sup>** anions.<sup>6</sup> Perhaps unsurprisingly, the toluene is held quite tightly within the framework: it is not removed

upon vacuum drying, and loss of solvent in the TGA is not complete until approximately 200 °C (Figure S29).

## Discussion

The crystal structures of the structures reported herein share several common features, which differentiate them from far more thoroughly-studied amidinium...carboxylate frameworks. While amidinium...carboxylate do show some variability in their hydrogen bonding arrangements, we have found that it is nearly always possible to isolate frameworks assembled only through  $R_2^2(8)$  hydrogen bonds between amidinium cations and carboxylate anions.<sup>26</sup> In contrast, in this work, a wide variety of hydrogen bonding interactions between amidinium and phosphonate groups is observed. This is particularly apparent in structures involving the tetrahedral phosphonate **phos<sub>tet</sub><sup>4-</sup>**. This wide variety of hydrogen bonding interactions is also reflected in phosphonate-containing structures adopting much lower symmetry space groups than the analogous amidinium...carboxylate and amidinium...sulfonate frameworks, which often crystallise in tetragonal space groups.<sup>21,22,25</sup> Part of the reason for this might be the length of the time taken to form crystals, as we have previously

observed that amidinium...carboxylate frameworks containing  $R_2^2(8)$  hydrogen bonds are kinetically-favoured products, which can rearrange to lower symmetry products if crystallisation is slowed.<sup>25</sup>

Another possibly surprising phenomenon is the influence of phosphonate...phosphonate hydrogen bonds, which are significantly shorter than amidinium...phosphonate hydrogen bonds. While these kind of anti-electrostatic hydrogen bonds are known to be significant in solution and in the solid state,<sup>32,34-36</sup> it is remarkable that the hydrogen bonds between two anionic species are shorter and apparently at least as important as a conventional electrostatic charge-assisted hydrogen bonding interaction between a cation and an anion. There are 18 of these phosphonate...phosphonate hydrogen bonds in the structures reported in this work (excluding the low quality high temperature data collection of **amid<sub>biphen</sub>·phos<sub>phen</sub>**) with a mean O...O distance of 2.543(11) Å, 85% of the sum of the van der Waals radii<sup>57</sup> of two oxygen atoms. These have either a D or  $R_2^2(8)$  geometry. Interactions with a D geometry are slightly shorter than those with an  $R_2^2(8)$  geometry (2.529(12) and 2.578(14) Å, respectively). Interestingly, this  $R_2^2(8)$  value is not significantly different than that observed for  $R_2^2(8)$  interactions between  $H_2PO_4^-$  anions in a previous survey of the Cambridge Structural Database (2.585(2) Å).<sup>31</sup> Amidinium...phosphonate hydrogen bonds are significantly longer (mean N...O distance of 2.859(19) Å, 94% of the sum of the van der Waals radii<sup>57</sup> of N and O, see Supporting Information for full analysis of hydrogen bonding parameters).

One of the initial motivations for investigating amidinium...phosphonate frameworks was that the additional hydrogen bonding interactions between phosphonate groups might give more robust frameworks than related amidinium...carboxylate or amidinium...sulfonate materials. This does not seem to be the case as **amid<sub>tet</sub>·phos<sub>tet</sub>** loses all crystallinity on thorough drying, as do the salts prepared from **amid<sub>phen</sub><sup>2+</sup>** or **amid<sub>biphen</sub><sup>2+</sup>** and **phos<sub>tet</sub><sup>4-</sup>**. This contrasts with frameworks prepared from **amid<sub>tet</sub><sup>4+</sup>** and the tetra-carboxylate or tetra-sulfonate analogues of **phos<sub>tet</sub><sup>4-</sup>**, which undergo structural rearrangements upon drying but remain crystalline (and which subsequently absorb water vapour).<sup>21,22,30</sup>

Other materials reported herein show significantly higher stability. For example, **amid<sub>biphen</sub>·phos<sub>phen</sub>** can retain crystallinity on losing solvent and (**guan**)<sub>2</sub>·**phos<sub>biphen</sub>** remains crystalline on drying and retains encapsulated toluene until approximately 200 °C. This suggests that the lack of stability of the amidinium...phosphonate structures involving **phos<sub>tet</sub><sup>4-</sup>** is not necessarily an innate feature of materials assembled through guanidinium/amidinium...phosphonate hydrogen bonds, but rather the structures of the specific networks. It is possible that more robust materials could be prepared from this building block, although we have studied a wide range of crystallisation conditions and not found such conditions. Crystal structure prediction<sup>58</sup> or high throughput screening<sup>23</sup>

approaches may offer ways to find stable, porous phases of these or related amidinium...phosphonate salts.

## Conclusions

We have prepared a series of hydrogen bonded frameworks from guanidinium or amidinium cations and polyphosphonates. A bis-amidinium crystallised with a diphosphonate to give a framework containing small water-filled channels: heating this caused a single-crystal-to-single-crystal transition to a close-packed anhydrous phase. Crystallisation of ditopic or tetratopic amidinium tectons with a tetrahedral phosphonate gave crystals containing relatively large water-filled channels, although these lost crystallinity upon thorough drying. Crystallisation of guanidinium cations with diphosphonate gave a structure related to, but distinct from, analogous guanidinium...sulfonate frameworks. In this structure, toluene is encapsulated in a pillared bilayer that has an overall anionic charge because it contains only one guanidinium cation for every diphosphonate. A second layer composed of guanidinium cations and solvent molecules gives a charge-neutral structure.

Generally we have found the rational design of amidinium...phosphonate frameworks to be challenging. We found it difficult to find crystallisation conditions to form the materials, and predicting hydrogen bonding geometries is not simple due to the multiple ways amidinium cations can interact with phosphonate anions, and phosphonate anions can interact with each other. While many of the materials prepared here are not particularly stable, we still think it likely that well-designed materials could have high stability due to the combination of inter- and intra-component hydrogen bonding.

## Experimental Section

### General remarks

The building blocks **amid<sub>phen</sub>·Cl<sub>2</sub>**,<sup>47</sup> **amid<sub>biphen</sub>·Cl<sub>2</sub>**,<sup>46</sup> **amid<sub>tet</sub>·Cl<sub>4</sub>**,<sup>21</sup> **phos<sub>phen</sub><sup>2H</sup>**,<sup>48</sup> **phos<sub>biphen</sub><sup>2H</sup>**,<sup>49</sup> and **phos<sub>tet</sub><sup>4H</sup>**<sup>50</sup> were prepared as previously described. Other compounds including solvents were purchased commercially and used as received. Characterisation data for new compounds and frameworks are provided in the SI.

### Synthesis of new compounds

**TBA<sub>2</sub>·phos<sub>biphen</sub>**: The diphosphonic acid **phos<sub>biphen</sub><sup>2H</sup>** (0.10 g, 0.32 mmol) was suspended in water (5 mL) and stirred under N<sub>2</sub> for 10 minutes at room temperature. TBA·OH (1.0 M, 0.72 mL, 0.72 mmol) was added and stirred for 10 minutes, during which time all material dissolved to give a brown solution. The reaction mixture was taken to dryness under reduced pressure to give a brown powder. Excess TBA·OH was removed by dissolving the crude material in warm acetone (2 mL) and precipitating with diethyl ether (8

mL). The resulting white powder was isolated by filtration, washed with diethyl ether ( $2 \times 10$  mL) and air-dried to give **TBA<sub>2</sub>·phos<sub>biphen</sub>**. Yield: 0.15 g (0.19 mmol, 59%).

<sup>1</sup>H NMR (D<sub>2</sub>O): 7.73–7.79 (m, 8H), 3.07–3.11 (m, 16H), 1.51–1.59 (m, 16H), 1.22–1.31 (m, 16H), 0.84 (t,  $J = 7.4$  Hz, 24H) ppm. <sup>13</sup>C{<sup>1</sup>H} NMR (D<sub>2</sub>O): 141.9, 134.6 (d,  $J = 178.2$  Hz), 131.0 (d,  $J = 10.2$  Hz), 126.9 (d,  $J = 14.3$  Hz), 58.1, 23.1, 19.1, 12.8 ppm. <sup>31</sup>P NMR (D<sub>2</sub>O): 12.9 ppm. ESI-MS (neg.): 313.011, calc. for [C<sub>12</sub>H<sub>11</sub>O<sub>6</sub>P<sub>2</sub>]<sup>-</sup>, i.e. [phos<sub>biphen</sub>]<sup>-</sup> = 313.004 Da.

**TBA<sub>4</sub>·phos<sub>tet</sub>**: The tetrakisphosphonic acid phos<sub>tet</sub><sup>4H</sup> (0.20 g, 0.31 mmol) was suspended in water (5 mL) and stirred under N<sub>2</sub> for 10 minutes at room temperature. TBA-OH in methanol (1.0 M, 1.4 mL, 1.4 mmol) was added and stirred for 10 minutes, during which time all material dissolved to give a brown solution. The reaction mixture was taken to dryness under reduced pressure to give a brown powder. Excess TBA-OH was removed by dissolving the brown powder in acetone (3 mL) and precipitating using diethyl ether (10 mL) to give a white powder. This was isolated by filtration, washed with diethyl ether ( $2 \times 10$  mL) and air-dried to give **TBA<sub>4</sub>·phos<sub>tet</sub>**. Yield: 0.41 g (0.26 mmol, 81%).

<sup>1</sup>H NMR (D<sub>2</sub>O): 7.52–7.58 (m, 8H), 7.36–7.38 (m, 8H), 3.08–3.12 (m, 32 H), 1.52–1.59 (m, 32H), 1.22–1.31 (m, 32 H), 0.85 (t,  $J = 7.4$  Hz, 48H) ppm. <sup>13</sup>C{<sup>1</sup>H} NMR (D<sub>2</sub>O): 148.4, 130.5 (d,  $J = 13.7$  Hz), 129.9 (d,  $J = 10.2$  Hz), 58.1, 23.1, 19.1, 12.8 ppm (2 peaks not observed). <sup>31</sup>P NMR (D<sub>2</sub>O): 12.7 ppm. ESI-MS (neg.): 560.280, calc. for [C<sub>57</sub>H<sub>92</sub>N<sub>2</sub>O<sub>12</sub>P<sub>4</sub>]<sup>2-</sup>, i.e. [TBA<sub>2</sub>·phos<sub>tet</sub>]<sup>2-</sup> = 560.281 Da.

**amid<sub>phen</sub>·phos<sub>phen</sub>**: A solution of phos<sub>phen</sub><sup>2H</sup> (4.8 mg, 20 μmol) in water (5 mL) was added to a solution of amid<sub>phen</sub>-Cl<sub>2</sub> (4.8 mg, 20 μmol) in water (5 mL). After several weeks standing at room temperature, colourless crystals formed. These were isolated by filtration, washed with water (3 mL) and dried under moderate vacuum. Yield: 4.7 mg (11 μmol, 55%). Yield calculated accounting for 2 H<sub>2</sub>O molecules per formula unit, as indicated by TGA and SCXRD.

<sup>1</sup>H NMR (d<sub>6</sub>-DMSO containing a drop of DCl<sub>(aq)</sub>): 9.78 (br. s, 4H), 9.45 (br. s, 4H), 8.05 (s, 8H), 7.73–7.77 (m, 4H). ATR-IR (*inter alia*): 1664 (br., C=N stretch), 1137 (P=O stretch) cm<sup>-1</sup>. TGA and PXRD data are provided in the SI.

**amid<sub>biphen</sub>·phos<sub>phen</sub>**: A solution of phos<sub>phen</sub><sup>2H</sup> (4.8 mg, 20 μmol) in water (10 mL) was added to a solution of amid<sub>biphen</sub>-Cl<sub>2</sub> (6.2 mg, 20 μmol) in water (10 mL). Within five minutes, colourless crystals formed. After two weeks, these were isolated by filtration, washed with water (3 mL) and dried under moderate vacuum. Yield: 5.7 mg (11 μmol, 55%). Yield calculated accounting for 2 H<sub>2</sub>O molecules per formula unit, as indicated by TGA and SCXRD.

<sup>1</sup>H NMR (d<sub>6</sub>-DMSO containing a drop of DCl<sub>(aq)</sub>): 9.65 (br. s, 4H), 9.39 (br. s, 4H), 8.05 (s, 8H), 7.75–7.79 (m, 4H). ATR-IR (*inter alia*): 1699 (br., C=N stretch), 1137 (P=O stretch) cm<sup>-1</sup>. TGA and PXRD data are provided in the SI.

**(amid<sub>phen</sub>)<sub>n</sub>·phos<sub>tet</sub>**: A solution of TBA<sub>4</sub>·phos<sub>tet</sub> (32 mg, 20 μmol) in 1:1 methanol:water (10 mL) was added to a solution of amid<sub>phen</sub>-Cl<sub>2</sub> (9.4 mg, 40 μmol) in 1:1 methanol:water (10 mL). After approximately a week, a few block-like crystals were visible. After 3 weeks, these were isolated by filtration, washed with water (6 mL) and dried under moderate vacuum. Yield: 1.5 mg. SCXRD unit cell analysis of 7 crystals showed they were all **(amid<sub>phen</sub>)<sub>2.5</sub>·phos<sub>tet</sub><sup>-1.5H</sup>**, however <sup>1</sup>H NMR analysis suggested the bulk material has an approximately 2:1 ratio of amid<sub>phen</sub><sup>2+</sup> to phos<sub>tet</sub><sup>4-</sup> (see SI for characterisation data).

**(amid<sub>biphen</sub>)<sub>n</sub>·phos<sub>tet</sub>**: A solution of TBA<sub>4</sub>·phos<sub>tet</sub> (10 mg, 6.5 μmol) in water (10 mL) was added to a solution of amid<sub>biphen</sub>-Cl<sub>2</sub> (6.4 mg, 20 μmol) in water (10 mL). After 2 days, a cloudy suspension containing needle-like crystals was observed, and over a few more weeks, the cloudiness cleared. After a month, the crystals were isolated by filtration, washed with water (6 mL) and dried under a moderate vacuum. Yield: 2.1 mg. SCXRD unit cell analysis of 8 crystals showed they were all **(amid<sub>biphen</sub>)<sub>3</sub>·phos<sub>tet</sub><sup>-2H</sup>**, however <sup>1</sup>H NMR analysis suggested the bulk material has an approximately 2:1 ratio of amid<sub>biphen</sub><sup>2+</sup> to phos<sub>tet</sub><sup>4-</sup> (see SI for characterisation data).

**amid<sub>tet</sub>·phos<sub>tet</sub>**: A solution of TBA<sub>4</sub>·phos<sub>tet</sub> (32.3 mg, 20.1 μmol) in water (10 mL) was added to a solution of amid<sub>tet</sub>-Cl<sub>4</sub> (12.7 mg, 20.0 μmol) in water (10 mL) resulting in the immediate formation of a cloudy suspension. Upon extended standing (~ 3 weeks), small needle-like crystals were observed and on further standing (~ 3 months), the cloudiness cleared to give a solution containing colourless crystals. These were isolated by filtration, washed with water (6 mL) and dried under moderate vacuum. Yield: 16.4 mg (13.1 μmol, 65%). Yield calculated accounting for 6 H<sub>2</sub>O molecules per formula unit, as indicated by TGA.

<sup>1</sup>H NMR (d<sub>6</sub>-DMSO containing a drop of DCl<sub>(aq)</sub>): 9.61 (br. s, 8H), 9.34 (br. s, 8H), 7.97 (d,  $J = 8.3$  Hz, 8H), 7.62–7.68 (m, 8H), 7.54 (d,  $J = 8.3$  Hz, 8H), 7.33 – 7.36 (m, 8H). ATR-IR (*inter alia*): 1675 (br., C=N stretch), 1130 (P=O stretch) cm<sup>-1</sup>. TGA and PXRD data are provided in the SI.

**(guan)<sub>2</sub>·phos<sub>biphen</sub>**: A solution of TBA<sub>2</sub>·phos<sub>biphen</sub> (16.3 mg, 21.2 μmol) in 1:1 methanol:toluene (40 mL) was added to a solution of guan-Cl (4.42 mg, 46.3 μmol) in 1:1 methanol:toluene (40 mL). After an extended period (~ 2 months), colourless plate-like crystals were observed. These were isolated by filtration and dried under moderate vacuum. Yield: 3.0 mg (6.3 μmol, 30%). Yield calculated accounting for half a molecule of toluene per formula unit, as indicated by <sup>1</sup>H NMR spectroscopy and TGA.

<sup>1</sup>H NMR (d<sub>6</sub>-DMSO containing a drop of DCl<sub>(aq)</sub>): 7.77 – 7.83 (m, 8H), 7.12 – 7.26 (m, 2.5H, toluene Ar-H), 2.29 (s, 1.5H, toluene CH<sub>3</sub>). ATR-IR (*inter alia*): 1655 (br., C=N

stretch), 1133 (P=O stretch)  $\text{cm}^{-1}$ . TGA and PXRD data are provided in the SI.

## Associated Content

**Supporting Information:** NMR and IR spectra, PXRD and TGA data, details of successful and unsuccessful crystallisations, details of X-ray crystallography including hydrogen bonding parameters.

**Accession codes:** CCDC 2371703 – 2371709 contain the supplementary crystallographic data for this paper.

## Notes

The authors declare no competing financial interest.

## Acknowledgements

We thank the Australian Research Council (PhD scholarship to PMN, FT210100495 to NGW) for funding and Dr Michael Gardiner for assistance with X-ray crystallography. Parts of this were conducted using the MX1<sup>59</sup> and MX2<sup>60</sup> beamlines of the Australian Synchrotron, and made use of the Australian Cancer Research Foundation detector.

## References

- Lin, R.-B.; He, Y.; Li, P.; Wang, H.; Zhou, W.; Chen, B. Multifunctional Porous Hydrogen-Bonded Organic Framework Materials. *Chem. Soc. Rev.* **2019**, *48*, 1362–1389. <https://doi.org/10.1039/C8CS00155C>.
- Yusov, A.; Dillon, A. M.; Ward, M. D. Hydrogen Bonded Frameworks: Smart Materials Used Smartly. *Mol. Syst. Des. Eng.* **2021**, *6*, 756–778. <https://doi.org/10.1039/D1ME00055A>.
- Ermer, O.; Lindenberg, L. Double-Diamond Inclusion Compounds of 2,6-Dimethylideneadamantane-1,3,5,7-Tetracarboxylic Acid. *Helv. Chim. Acta* **1991**, *74* (4), 825–877. <https://doi.org/10.1002/hlca.19910740417>.
- Simard, M.; Su, D.; Wuest, J. D. Use of Hydrogen Bonds to Control Molecular Aggregation. Self-Assembly of Three-Dimensional Networks with Large Chambers. *J. Am. Chem. Soc.* **1991**, *113* (12), 4696–4698. <https://doi.org/10.1021/ja00012a057>.
- Wang, X.; Simard, M.; Wuest, J. D. Molecular Tectonics. Three-Dimensional Organic Networks with Zeolitic Properties. *J. Am. Chem. Soc.* **1994**, *116* (26), 12119–12120. <https://doi.org/10.1021/ja00105a089>.
- Russell, V. A.; Evans, C. C.; Li, W.; Ward, M. D. Nanoporous Molecular Sandwiches: Pillared Two-Dimensional Hydrogen-Bonded Networks with Adjustable Porosity. *Science* **1997**, *276* (5312), 575–579. <https://doi.org/10.1126/science.276.5312.575>.
- Holman, K. T.; Pivovar, A. M.; Swift, J. A.; Ward, M. D. Metric Engineering of Soft Molecular Host Frameworks. *Acc. Chem. Res.* **2001**, *34* (2), 107–118. <https://doi.org/10.1021/ar970272f>.
- Horner, M. J.; Holman, K. T.; Ward, M. D. Architectural Diversity and Elastic Networks in Hydrogen-Bonded Host Frameworks: From Molecular Jaws to Cylinders. *J. Am. Chem. Soc.* **2007**, *129* (47), 14640–14660. <https://doi.org/10.1021/ja0741574>.
- Adachi, T.; Ward, M. D. Versatile and Resilient Hydrogen-Bonded Host Frameworks. *Acc. Chem. Res.* **2016**, *49* (12), 2669–2679. <https://doi.org/10.1021/acs.accounts.6b00360>.
- Yang, W.; Greenaway, A.; Lin, X.; Matsuda, R.; Blake, A. J.; Wilson, C.; Lewis, W.; Hubberstey, P.; Kitagawa, S.; Champness, N. R.; Schröder, M. Exceptional Thermal Stability in a Supramolecular Organic Framework: Porosity and Gas Storage. *J. Am. Chem. Soc.* **2010**, *132* (41), 14457–14469. <https://doi.org/10.1021/ja1042935>.
- Mastalerz, M.; Oppel, I. M. Rational Construction of an Extrinsic Porous Molecular Crystal with an Extraordinary High Specific Surface Area. *Angew. Chem. Int. Ed.* **2012**, *51* (21), 5252–5255. <https://doi.org/10.1002/anie.201201174>.
- Pulido, A.; Chen, L.; Kaczorowski, T.; Holden, D.; Little, M. A.; Chong, S. Y.; Slater, B. J.; McMahon, D. P.; Bonillo, B.; Stackhouse, C. J.; Stephenson, A.; Kane, C. M.; Clowes, R.; Hasell, T.; Cooper, A. I.; Day, G. M. Functional Materials Discovery Using Energy–Structure–Function Maps. *Nature* **2017**, *543*, 657–664. <https://doi.org/10.1038/nature21419> <https://www.nature.com/articles/nature21419#supplementary-information>.
- Ma, K.; Li, P.; Xin, J. H.; Chen, Y.; Chen, Z.; Goswami, S.; Liu, X.; Kato, S.; Chen, H.; Zhang, X.; Bai, J.; Wasson, M. C.; Maldonado, R. R.; Snurr, R. Q.; Farha, O. K. Ultrastable Mesoporous Hydrogen-Bonded Organic Framework-Based Fiber Composites toward Mustard Gas Detoxification. *Cell Rep. Phys. Sci.* **2020**, *1* (2), 100024. <https://doi.org/10.1016/j.xcrp.2020.100024>.
- Yang, Y.; Li, L.; Lin, R.-B.; Ye, Y.; Yao, Z.; Yang, L.; Xiang, F.; Chen, S.; Zhang, Z.; Xiang, S.; Chen, B. Ethylene/Ethane Separation in a Stable Hydrogen-Bonded Organic Framework through a Gating Mechanism. *Nat. Chem.* **2021**. <https://doi.org/10.1038/s41557-021-00740-z>.
- Hisaki, I.; Suzuki, Y.; Gomez, E.; Ji, Q.; Tohrai, N.; Nakamura, T.; Douhal, A. Acid Responsive Hydrogen-Bonded Organic Frameworks. *J. Am. Chem. Soc.* **2019**, *141* (5), 2111–2121. <https://doi.org/10.1021/jacs.8b12124>.
- Huang, Q.; Chen, X.; Li, W.; Yang, Z.; Zhang, Y.; Zhao, J.; Chi, Z. Local Dynamics in a Hydrogen-Bonded Organic Framework for Adaptive Guest Accommodation with Programmable Luminescence. *Chem* **2023**, *9* (5), 1241–1254. <https://doi.org/10.1016/j.chempr.2023.01.013>.
- Liang, W.; Carraro, F.; Solomon, M. B.; Bell, S. G.; Amenitsch, H.; Sumbly, C. J.; White, N. G.; Falcaro, P.; Doonan, C. J. Enzyme Encapsulation in a Porous Hydrogen-Bonded Organic Framework. *J. Am. Chem. Soc.* **2019**, *141* (36), 14298–14305. <https://doi.org/10.1021/jacs.9b06589>.
- Chen, G.; Huang, S.; Shen, Y.; Kou, X.; Ma, X.; Huang, S.; Tong, Q.; Ma, K.; Chen, W.; Wang, P.; Shen, J.; Zhu, F.; Ouyang, G. Protein-Directed, Hydrogen-Bonded Biohybrid Framework. *Chem* **2021**, *7* (10), 2722–2742. <https://doi.org/10.1016/j.chempr.2021.07.003>.
- Chen, X.-Y.; Cao, L.-H.; Bai, X.-T.; Cao, X.-J. Charge-Assisted Ionic Hydrogen-Bonded Organic Frameworks: Designable and Stabilized Multifunctional Materials. *Chem. Eur. J.* **2024**, *30* (17), e202303580. <https://doi.org/10.1002/chem.202303580>.
- Xing, G.; Peng, D.; Ben, T. Crystalline Porous Organic Salts. *Chem. Soc. Rev.* **2024**, *53* (3), 1495–1513. <https://doi.org/10.1039/D3CS00855J>.
- Boer, S. A.; Conte, L.; Tarzia, A.; Huxley, M. T.; Gardiner, M. G.; Appadoo, D. R. T.; Ennis, C.; Doonan, C. J.; Richardson, C.; White, N. G. Water Sorption Controls Extreme Single-Crystal-to-Single-Crystal Molecular Reorganization in Hydrogen Bonded Organic Frameworks. *Chem. Eur. J.* **2022**, *28* (57), e202201929. <https://doi.org/10.1002/chem.202201929>.
- Muang-Non, P.; Richardson, C.; White, N. G. Correspondence on “Crystalline Porous Organic Salt for Ultrarapid Adsorption/Desorption-Based Atmospheric Water Harvesting by Dual Hydrogen Bond System.” *Angew. Chem. Int. Ed.* **2023**, *62* (8), e202212962. <https://doi.org/10.1002/anie.202212962>.
- O’Shaughnessy, M.; Padgham, A. C.; Clowes, R.; Little, M. A.; Brand, M. C.; Qu, H.; Slater, A. G.; Cooper, A. I. Controlling the Crystallisation and Hydration State of Crystalline Porous Organic Salts. *Chem. Eur. J.* **2023**, *29* (64), e202302420. <https://doi.org/10.1002/chem.202302420>.
- Wahl, H.; Haynes, D. A.; le Roex, T. Porous Salts Based on the Pamoate Ion. *Chem. Commun.* **2012**, *48* (12), 1775–1777. <https://doi.org/10.1039/C2CC14753J>.

- (25) Morshedi, M.; Thomas, M.; Tarzia, A.; Doonan, C. J.; White, N. G. Supramolecular Anion Recognition in Water: Synthesis of Hydrogen-Bonded Supramolecular Frameworks. *Chem. Sci.* **2017**, *8* (4), 3019–3025. <https://doi.org/10.1039/C7SC00201G>.
- (26) White, N. G. Amidinium...carboxylate Frameworks: Predictable, Robust, Water-Stable Hydrogen Bonded Materials. *Chem. Commun.* **2021**, 57 (84), 10998–11008. <https://doi.org/10.1039/D1CC04782E>.
- (27) Miyano, T.; Okada, N.; Nishida, R.; Yamamoto, A.; Hisaki, I.; Tohnai, N. A Structurally Variable Porous Organic Salt Based on a Multidirectional Supramolecular Cluster. *Chem. Eur. J.* **2016**, *22* (43), 15430–15436. <https://doi.org/doi:10.1002/chem.201602233>.
- (28) Xing, G.; Yan, T.; Das, S.; Ben, T.; Qiu, S. Synthesis of Crystalline Porous Organic Salts with High Proton Conductivity. *Angew. Chem. Int. Ed.* **2018**, *57* (19), 5345–5349. <https://doi.org/10.1002/anie.201800423>.
- (29) Xing, G.; Bassanetti, I.; Bracco, S.; Negroni, M.; Bezuidenhout, C.; Ben, T.; Sozzani, P.; Comotti, A. A Double Helix of Opposite Charges to Form Channels with Unique CO<sub>2</sub> Selectivity and Dynamics. *Chem. Sci.* **2019**, *10*, 730–736. <https://doi.org/10.1039/C8SC04376K>.
- (30) Zhang, S.; Fu, J.; Das, S.; Ye, K.; Zhu, W.; Ben, T. Crystalline Porous Organic Salt for Ultrarapid Adsorption/Desorption-Based Atmospheric Water Harvesting by Dual Hydrogen Bond System. *Angew. Chem. Int. Ed.* **2022**, *61* (40), e202208660. <https://doi.org/10.1002/anie.202208660>.
- (31) White, N. G. Antielectrostatically Hydrogen Bonded Anion Dimers: Counterintuitive, Common and Consistent. *CrystEngComm* **2019**, *21*, 4855–4858.
- (32) Zhao, W.; Flood, A. H.; White, N. G. Recognition and Applications of Anion–Anion Dimers Based on Anti-Electrostatic Hydrogen Bonds (AEHBs). *Chem. Soc. Rev.* **2020**, *49* (22), 7893–7906. <https://doi.org/10.1039/D0CS00486C>.
- (33) Cullen, D. A.; Gardiner, M. G.; White, N. G. A Three Dimensional Hydrogen Bonded Organic Framework Assembled through Antielectrostatic Hydrogen Bonds. *Chem. Commun.* **2019**, 55 (80), 12020–12023. <https://doi.org/10.1039/C9CC06707H>.
- (34) Zhao, W.; Qiao, B.; Chen, C.-H.; Flood, A. H. High-Fidelity Multistate Switching with Anion–Anion and Acid–Anion Dimers of Organophosphates in Cyanostar Complexes. *Angew. Chem. Int. Ed.* **2017**, *56* (42), 13083–13087. <https://doi.org/10.1002/anie.201707869>.
- (35) Fatila, E. M.; Pink, M.; Twum, E. B.; Karty, J. A.; Flood, A. H. Phosphate–Phosphate Oligomerization Drives Higher Order Co-Assemblies with Stacks of Cyanostar Macrocycles. *Chem. Sci.* **2018**, *9* (11), 2863–2872. <https://doi.org/10.1039/C7SC05290A>.
- (36) Zhao, W.; Qiao, B.; Tropp, J.; Pink, M.; Azoulay, J. D.; Flood, A. H. Linear Supramolecular Polymers Driven by Anion–Anion Dimerization of Difunctional Phosphonate Monomers Inside Cyanostar Macrocycles. *J. Am. Chem. Soc.* **2019**, *141* (12), 4980–4989. <https://doi.org/10.1021/jacs.9b00248>.
- (37) Göbel, M. W.; Bats, J. W.; Dürner, G. En Route to Synthetic Phosphodiesterases: Supramolecular Phosphoryl-Transfer Mediated by Amidinium–Phosphate Contact Ion-Pairs. *Angew. Chem. Int. Ed. Engl.* **1992**, *31* (2), 207–209. <https://doi.org/10.1002/anie.199202071>.
- (38) Kusakawa, T.; Nagano, H.; Nakaguchi, K.; Takeshita, S.; Harumoto, Y. Turn-on Fluorescence Sensor for Mono- and Di-Phosphonic Acid Derivatives Using Anthracene-Based Diamidine and Its Detection of Amidinium-Phosphonate and Amidinium Formation. *Tetrahedron* **2018**, *74* (4), 465–476. <https://doi.org/10.1016/j.tet.2017.12.011>.
- (39) Kusakawa, T.; Nakaguchi, K.; Nishimura, S.; Nakajima, A. Recognition of Dicarboxylic Acids and Diphosphonic Acids Using Anthracene-Based Diamidine: Formation of Amidinium-Carboxylate and Amidinium-Phosphonate Salt Bridges in a Protic Solvent. *Supramol. Chem.* **2021**, *33* (3), 43–52. <https://doi.org/10.1080/10610278.2021.1908545>.
- (40) Lie, S.; Maris, T.; Wuest, J. D. Molecular Networks Created by Charge-Assisted Hydrogen Bonding in Phosphonate, Phosphate, and Sulfonate Salts of Bis(Amidines). *Cryst. Growth Des.* **2014**, *14* (7), 3658–3666. <https://doi.org/10.1021/cg500726v>.
- (41) Zheng, S.; Li, L.; Chen, L.; Fan, Z.; Xiang, F.; Yang, Y.; Zhang, Z.; Xiang, S. Two Water Stable Phosphate-Amidinium Based Hydrogen-Bonded Organic Framework with Proton Conduction. *Z. Für Anorg. Allg. Chem.* **2022**, *648* (12), e202200031. <https://doi.org/10.1002/zaac.202200031>.
- (42) Almuhana, A. R. Y.; Griffin, S. L.; Champness, N. R. Amidinium...Phosphonate Charge Assisted Hydrogen-bonded Organic Frameworks: Influence of Diverse Intermolecular Interactions. *CrystEngComm* **2024** DOI: 10.1039/d4ce00479e.
- (43) Sopkova-de Oliveira Santos, J.; Montouillout, V.; Fayon, F.; Fernandez, C.; Delain-Bioton, L.; Villemin, D.; Jaffrès, P.-A. Assembly of Benzene-1,3,5-Tris(Methylenephosphonic Acid) and Guanidinium Salt: Single Crystal-X-Ray Characterisation and <sup>31</sup>P Solid State NMR Investigations. *New J. Chem.* **2004**, *28* (10), 1244–1249. <https://doi.org/10.1039/B406938B>.
- (44) Yang, J.; Yin, J.; Guo, Q.; Xie, C.; Yang, Q.; Kong, Z.; Kang, Z.; Wang, R.; Sun, D. Guest-Induced Proton Conductivity of Two-Dimensional Layered Hydrogen-Bonded Organic Frameworks. *Inorg. Chem. Front.* **2023**, *10* (21), 6262–6268. <https://doi.org/10.1039/D3QI01401K>.
- (45) Bernstein, J.; Davis, R. E.; Shimoni, L.; Chang, N.-L. Patterns in Hydrogen Bonding: Functionality and Graph Set Analysis in Crystals. *Angew. Chem. Int. Ed.* **1995**, *34* (15), 1555–1573. <https://doi.org/doi:10.1002/anie.199515551>.
- (46) Tzioumis, N. A.; Cullen, D. A.; Jolliffe, K. A.; White, N. G. Selective Removal of Sulfate from Water by Precipitation with a Rigid Bis-Amidinium Compound. *Angew. Chem. Int. Ed.* **2023**, *62* (12), e202218360. <https://doi.org/10.1002/anie.202218360>.
- (47) Wang, K.; Yang, L.-M.; Wang, X.; Guo, L.; Cheng, G.; Zhang, C.; Jin, S.; Tan, B.; Cooper, A. Covalent Triazine Frameworks via a Low-Temperature Polycondensation Approach. *Angew. Chem. Int. Ed.* **2017**, *56* (45), 14149–14153. <https://doi.org/10.1002/anie.201708548>.
- (48) Amghouz, Z.; García-Granda, S.; García, J. R.; Clearfield, A.; Valiente, R. Organic–Inorganic Hybrids Assembled from Lanthanide and 1,4-Phenylenebis(Phosphonate). *Cryst. Growth Des.* **2011**, *11* (12), 5289–5297. <https://doi.org/10.1021/cg2008254>.
- (49) Wang, Z.; Heising, J. M.; Clearfield, A. Sulfonated Microporous Organic–Inorganic Hybrids as Strong Bronsted Acids <sup>1</sup>. *J. Am. Chem. Soc.* **2003**, *125* (34), 10375–10383. <https://doi.org/10.1021/ja030226c>.
- (50) Zareba, J. K.; Biatek, M. J.; Janczak, J.; Zoń, J.; Dobosz, A. Extending the Family of Tetrahedral Tectons: Phenyl Embraces in Supramolecular Polymers of Tetraphenylmethane-Based Tetraphosphonic Acid Templated by Organic Bases. *Cryst. Growth Des.* **2014**, *14* (11), 6143–6153. <https://doi.org/10.1021/cg501348g>.
- (51) In this and other cases in this paper, more complex graph set notation could be used to describe the hydrogen bonding, e.g. this C(4) chain hydrogen bonding could be considered as two chains (both phosphonate...phosphonate interactions) made up of rings. In the interests of simplicity, we do not use this level of analysis.
- (52) Franz, R. G. Comparisons of pK<sub>a</sub> and Log P Values of Some Carboxylic and Phosphonic Acids: Synthesis and Measurement. *AAPS PharmSci* **2001**, *3* (2), 10. <https://doi.org/10.1208/ps030210>.
- (53) Spek, A. L. PLATON SQUEEZE: A Tool for the Calculation of the Disordered Solvent Contribution to the Calculated Structure Factors. *Acta Crystallogr.* **2015**, *C71*, 9–18. <https://doi.org/10.1107/S2053229614024929>.
- (54) Dolomanov, O. V.; Bourhis, L. J.; Gildea, R. J.; Howard, J. A. K.; Puschmann, H. OLEX2: A Complete Structure Solution, Refinement and Analysis Program. *J. Appl. Crystallogr.* **2009**, *42*, 339–341. <https://doi.org/10.1107/S0021889808042726>.
- (55) Adachi, T.; Ward, M. D. Versatile and Resilient Hydrogen-Bonded Host Frameworks. *Acc. Chem. Res.* **2016**, *49*, 2669–2679. <https://doi.org/10.1021/acs.accounts.6b00360>.
- (56) Swift, J. A.; Reynolds, A. M.; Ward, M. D. Cooperative Host–Guest Recognition in Crystalline Clathrates: Steric Guest Ordering by Molecular Gears. *Chem. Mater.* **1998**, *10* (12), 4159–4168. <https://doi.org/10.1021/cm980600l>.
- (57) Alvarez, S. A Cartography of the van Der Waals Territories. *Dalton Trans.* **2013**, *42* (24), 8617–8636. <https://doi.org/10.1039/c3dt50599e>.

- (58) O'Shaughnessy, M.; Glover, J.; Hafizi, R.; Barhi, M.; Clowes, R.; Chong, S. Y.; Argent, S. P.; Day, G. M.; Cooper, A. I. Porous Isorecticular Non-Metal Organic Frameworks. *Nature* **2024**, *630* (8015), 102–108. <https://doi.org/10.1038/s41586-024-07353-9>.
- (59) Cowieson, N. P.; Aragao, D.; Clift, M.; Ericsson, D. J.; Gee, C. H.; Mudie, N.; Panjikar, S.; Price, J. R.; Riboldi-Tunnicliffe, A.; Williamson, R.; Caradoc-Davies, T. MX1: A Bending-Magnet Crystallography Beamline Serving Both Chemical and Macromolecular Crystallography Communities at the Australian Synchrotron. *J. Synchrotron Radiat.* **2015**, *22*, 187–190. <https://doi.org/10.1107/S1600577514021717>.
- (60) Aragao, D.; Aishima, J.; Cherukuvada, H.; Clarken, R.; Clift, M.; Cowieson, N. P.; Ericsson, D. J.; Gee, C. L.; Macedo, S.; Mudie, N.; Panjikar, S.; Price, J. R.; Riboldi-Tunnicliffe, A.; Rostan, R.; Williamson, R.; Caradoc-Davies, T. T. MX2: A High-Flux Undulator Microfocus Beamline Serving Both the Chemical and Macromolecular Crystallography Communities at the Australian Synchrotron. *J. Synchrotron Radiat.* **2018**, *25* (3), 885–891. <https://doi.org/doi:10.1107/S1600577518003120>.